



INFLUENCE OF THE PROCESS PARAMETERS ON THE MICRO-HARDNESS OBTAINED OF DIAMOND BURNISHED AISI 304L STAINLESS STEEL

Angel Anchev*

Technical University of Gabrovo, 5300 Gabrovo, Bulgaria

ARTICLE INFO

Article history:

Received 6 March 2022

Accepted 23 March 2022

Keywords:

chromium-nickel austenitic stainless steels; diamond burnishing; micro-hardness; strain-induced martensite

ABSTRACT

Chromium-nickel austenitic stainless steels are used in many industrial fields due to their good strength, excellent corrosion resistance, easy deformation in the plastic field and good weldability. Their low hardness, poor tribological properties and the possibility of localized corrosion in specific environments may limit their use. In the temperature range 500-700°C these steels are vulnerable to inter-granular corrosion. As a result, the conventional chemical-thermal treatments, such as nitriding and carburizing, can increase the surface hardness, but at the expense of the corrosion resistance due to the formation of chromium carbides. This disadvantage is overcome by low-temperature nitriding and carburization, which are realized at temperatures below 500 °C, but these treatments are relatively expensive. As is well known, the austenite is easily hardened by cold plastic deformation. With a higher degree of plastic deformation, the austenite partially turns into alpha prime strain-induced martensite, where the hardness increases significantly. The article presents results for the surface micro-hardness of AISI 304L cylindrical steel specimens treated with diamond burnishing, which is a cheap green technology. The surface cold work was performed on C11 conventional lathe using a burning device with elastic fixation of the deforming polycrystalline diamond insert. The micro-hardness obtained after a previous fine turning of 366 HV0.05 was increased to 609 HV0.05 via diamond burnishing, i.e., the increase is 66.4%.

© 2022 Journal of the Technical University of Gabrovo. All rights reserved.

1. INTRODUCTION

Chromium-nickel austenitic stainless steels are used in many industrial fields due to their good strength, excellent corrosion resistance, easy deformation in the plastic field and good weldability. Their low hardness, poor tribological properties and the possibility of localized corrosion in specific environments may limit their use. In the temperature range 500-700 °C these steels are vulnerable to intergranular corrosion [1]. As a result, the conventional chemical-thermal treatments, such as nitriding and carburizing, can increase the surface hardness, but at the expense of the corrosion resistance due to the formation of chromium carbides. This disadvantage is overcome by low-temperature nitriding [2-5] and carburization [6], which are realized at temperatures below 500 °C, but these treatments are relatively expensive. As is well known, the austenite is easily hardened by cold plastic deformation. With a higher degree of plastic deformation, the austenite partially turns into alpha prime strain-induced martensite, where the hardness increases significantly [7-20]. Plastic deformation is introduced via cold rolling [7, 8, 10-12, 14, 15, 17], via cold rolling and sandblasting [16], by torsion under high pressure [18], due to fatigue tests with stress amplitude in the plastic field [20]. There is no information in the literature on the transformation of austenite to alpha prime martensite in the surface layer caused by burnishing. This

type of finishing has been applied to improve the surface integrity characteristics of austenitic stainless steels. Dyl et al. [21] studied the effect of slide burnishing on roughness obtained of 314L stainless steel sleeves. Shi et al. [22] improved the surface integrity of austenitic stainless steel via ultrasonic burnishing using two types of burnishing tips. Modeling of surface microhardness of slide diamond burnished AISI 304 steel was performed by Varga and Ferencsik [23]. Konefal et al. [24] improved the corrosion resistance of AISI 316Ti austenitic stainless steel via diamond burnishing. Equilibrium surface texture of valve stems made of austenitic stainless steel AISI 317Ti was obtained by Korzynski et al. [25] via slide diamond burnishing. Korzynski et al. [26] established the correlations between surface parameters of the same steel after slide diamond burnishing. Maximov et al. [27] studied the effect of diamond burnishing on surface integrity and performance behaviour of AISI 316Ti chromium-nickel austenitic steel. Slide burnishing with a rotary tool was applied on AISI 316 steel by Okada et al. [28]. These authors studied the effect of slide burnishing on the characteristics of surface integrity. However, there is no information concerning strain-induced alpha prime martensite due to burnishing. Achieving such a transformation through burnishing will significantly

* Corresponding author. E-mail: anchev@mail.bg

increase the surface micro-hardness of austenitic chromium-nickel stainless steels.

The main objective of this article is to achieve maximum surface micro-hardness of AISI 304L stainless steel via slide diamond burnishing due to availability of strain-induced alpha prime martensite in the surface layer.

2. MATERIALS AND METHODS

2.1. Material

The material used was AISI 304L chromium-nickel austenitic stainless steels and was obtained as cylindrical bars with diameters of, respectively 30 and 70 mm. Chemical analysis and mechanical testing were conducted.

Table 1 Chemical composition of the received steel

Fe	C	Si	Mn	P	S	Cr	Mo	Ni	Co	Cu
70.4	0.0388	0.237	1.63	0.0393	0.0448	17.7	0.26	8.76	0.136	0.499

2.2. Diamond burnishing implementation

The diamond burnishing was performed on C11 conventional lathe using a burning device with elastic fixation of the deforming polycrystalline diamond insert (Fig. 1). A lubricant – cooler Hacut 795-H was used. The cylindrical specimens had diameters in the 16-68 mm range. Turning as premachining and slide burnishing were carried out in one clamping process to minimize the concentric run-out in burnishing. The turning was conducted from end to end of each specimen, while the treated length through slide burnishing with one combination of governing factors was 20 mm. Thus, for a group of experimental points (combinations of governing factors) one and the same initial roughness before burnishing was ensured.

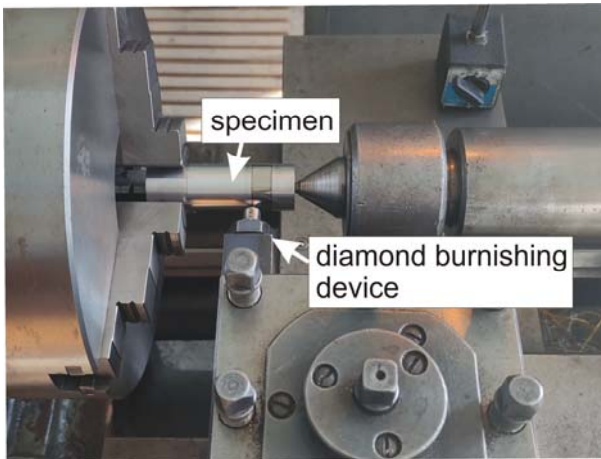


Fig. 1. Diamond burnishing implementation on C11 lathe

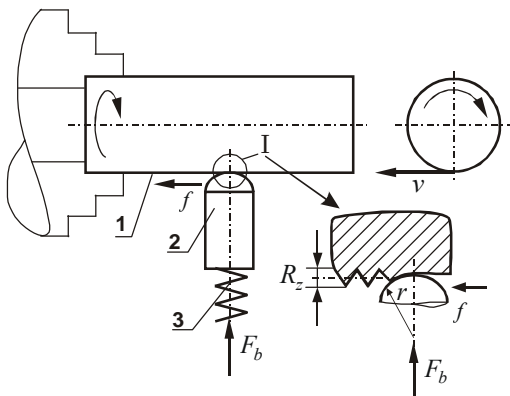


Fig. 2. Illustration of the diamond burnishing parameters

The chemical composition is shown in Table 1. The mechanical characteristics at room temperature of this steel (“as received”) were established as follows: yield limit $R_{0.2} = 418 \text{ MPa}$, ultimate stress $R_m = 707 \text{ MPa}$, elongation $A_5 = 36.5\%$, transverse contraction $Z = 72.4\%$, hardness 245 HB and impact toughness 185 J/cm^2 .

All subsequent treatments with diamond burnishing were performed on AISI 304L steel in “as received” state, i.e., without prior heat treatment.

The governing factors of the slide burnishing process are the following: sphere radius of the diamond insert $r, \text{ mm}$; burnishing force $F_b, \text{ N}$; feed rate $f, \text{ mm/rev}$; burnishing velocity $v, \text{ m/min}$ and number of passes n (Fig. 2).

2.3. Surface micro-hardness measurement

The surface micro-hardness $HV_{0.05}$ measurements were conducted via a ZHV μ Zwick/Roell micro-hardness tester featuring computerized processing of the measurement results and using a load of 0.05 kgf and a holding time of 10 s . Twenty-four measurements were made for each experimental point. The final value of the surface micro-hardness at each point was taken to be their group center.

2.4. Basic method of study

The basic method of study was one-factor-at-a-time. When studying the influence of a factor on the surface micro-hardness, this factor changes at a certain interval (constant or variable), and the other factors are maintained at constant levels.

3. RESULTS AND DISCUSSION

3.1. Influence of the process parameters on the surface micro-hardness

The effect of the specimen diameter d in the $(16 - 68) \text{ mm}$ range on the surface micro-hardness is shown in Fig. 3. The surface micro-hardness obtained alters in $(400 - 432) \text{ HV}_{0.05}$ range. There is no stable unambiguous trend. The increased surface micro-hardness is a consequence of hardening of surface deformation, i.e., the greater the equivalent plastic deformation of the surface layer, the greater the surface micro-hardness. Obviously, when $d = 30 \text{ mm}$ and $r = 3 \text{ mm}$ the greatest equivalent plastic deformation of the surface layer is obtained, and hence the greatest micro-hardness.

The effect of the burnishing velocity on the surface micro-hardness is shown in Fig. 4. In the speed range $(50 - 425) \text{ m/min}$ the measured micro-hardness varies from 396 to 409HV. It can be concluded that the burnishing velocity has a small effect on the resulting micro-hardness for this steel.

The effect of the feed rate on the surface micro-hardness is shown in Fig. 5. Evidently, the feed rate influences strongly on the micro-hardness. The smallest feed leads to the greatest micro-hardness, due to the so-called overlapping effect.

The effect of the number of passes on the surface micro-hardness is shown in Fig. 6. A steady trend is observed to increase the micro-hardness when the passes increase from one to five. A similar trend, but less pronounced, is observed with a further increase in passes to eight. Diamond burnishing causes cyclic loading in vicinity of each point from the surface layer. Probably at $n=5$ a stabilized cycle is reached and for a further increase in the number of passes the micro-hardness changes slightly. Detailed information on achieving a stabilized cycle in the diamond burnishing process is given in [29].

The effect of the radius and burnishing force on the surface micro-hardness is shown in Fig. 7. Obviously, the radius has a greater effect on the surface micro-hardness

than the burning force. The highest micro-hardness is obtained using $r = 2\text{mm}$ for all values of burnishing force. The other two values of the radius - 3 and 4 mm, lead to practically equal values of the micro-hardness for all applied values of burnishing force. In order to obtain maximum surface micro-hardness, it is not advisable for the burning force to exceed 600 N. Increasing the burning force leads to an increase in the equivalent plastic deformation in the contact zone with the deforming diamond insert. Obviously, the combination of radius and burnishing force, which leads to maximum equivalent plastic deformation of the specimen surface, provides maximum surface micro-hardness. A further increase in burnishing force will increase the depth of the plastic area and shift the maximum equivalent deformation at points below the surface layer. This explains the decrease in surface micro-hardness when the burning force increases above 600 N.

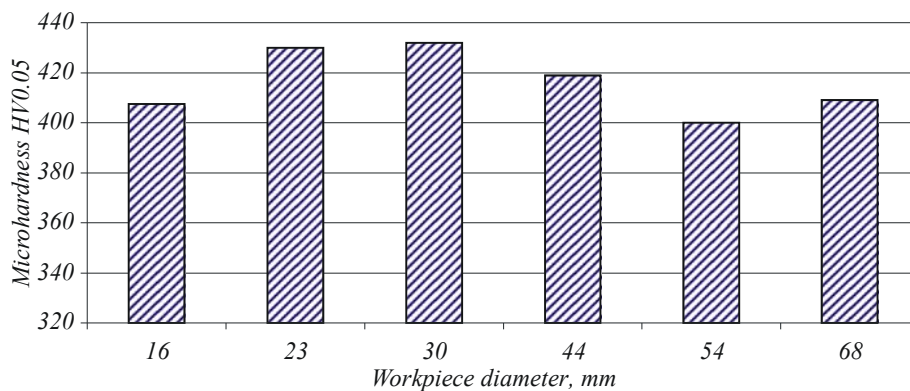


Fig. 3. Effect of the specimen diameter on the surface micro-hardness: $r = 3\text{mm}$; $F_b = 150\text{N}$; $f = 0.07\text{mm/rev}$; $v = 50\text{m/min}$; $n = 1$

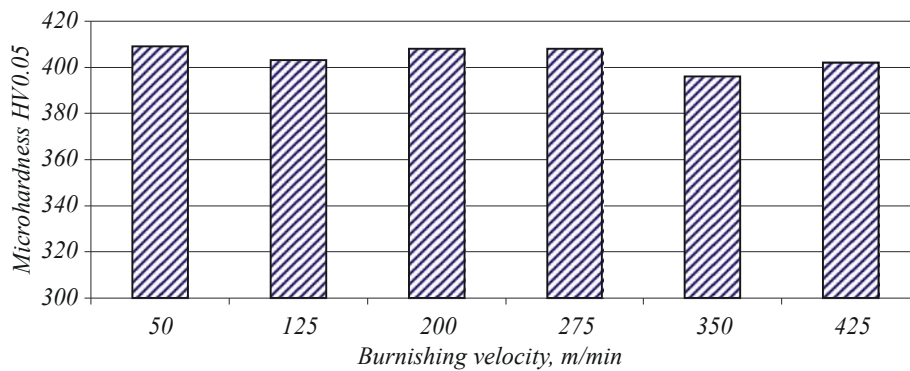


Fig. 4. Effect of the burnishing velocity on the surface micro-hardness: $r = 3\text{mm}$; $F_b = 150\text{N}$; $f = 0.07\text{mm/rev}$; $n = 1$; $d = 68\text{mm}$

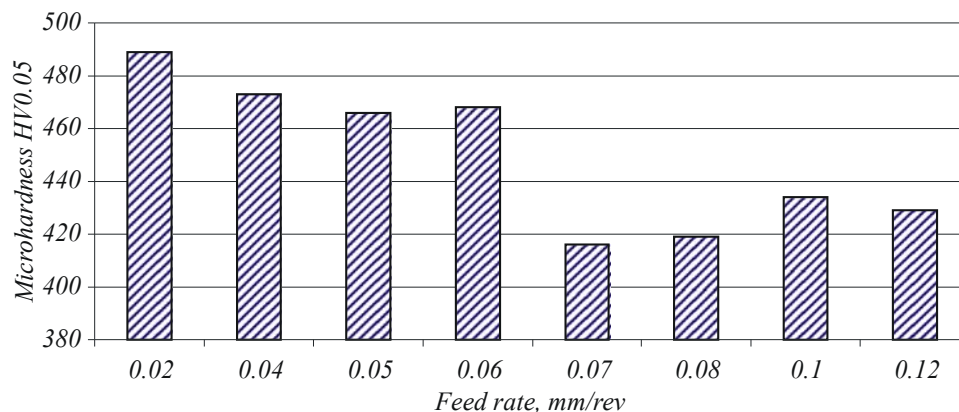


Fig. 5. Effect of the feed rate on the surface micro-hardness: $r = 3\text{mm}$; $F_b = 300\text{N}$; $v = 100\text{m/min}$; $n = 1$; $d = 29\text{mm}$

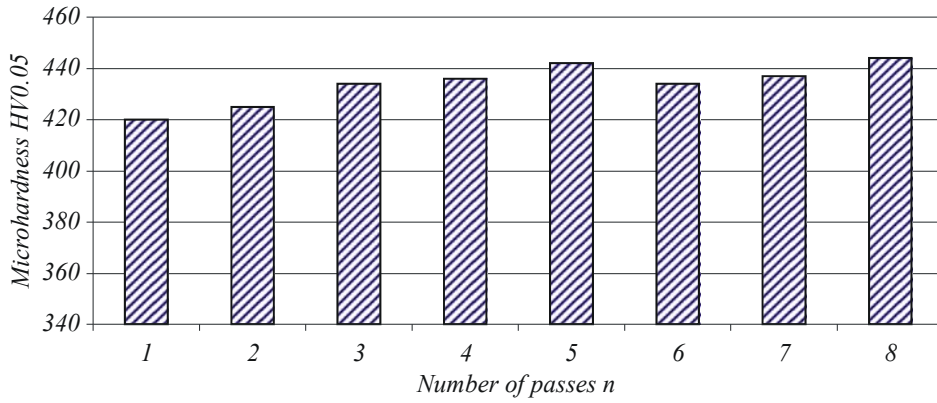


Fig. 6. Effect of the number of passes on the surface micro-hardness:
 $r = 3\text{mm}$; $F_b = 300\text{N}$; $f = 0.07\text{mm / rev}$; $v = 100\text{m / min}$; $d = 28\text{mm}$

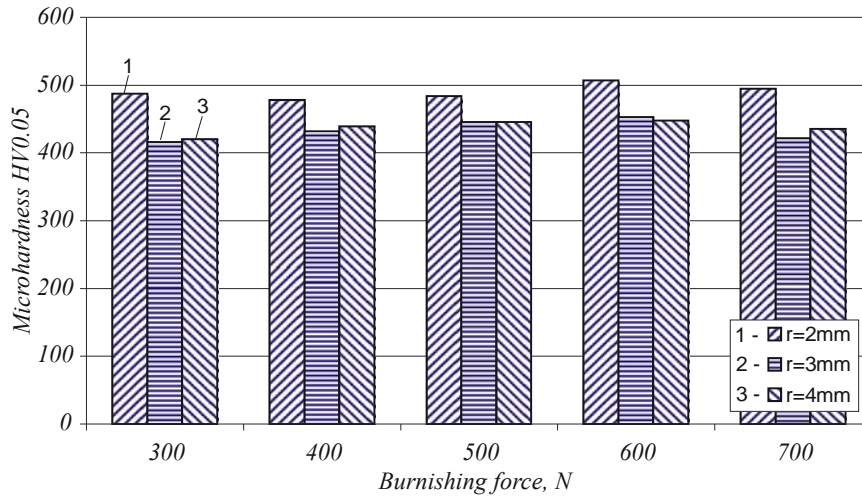


Fig. 7. Effect of the radius and burnishing force on the surface micro-hardness:
 $f = 0.07\text{mm / rev}$; $v \approx 60\text{m / min}$; $n = 1$; $d = (23 - 29)\text{mm}$

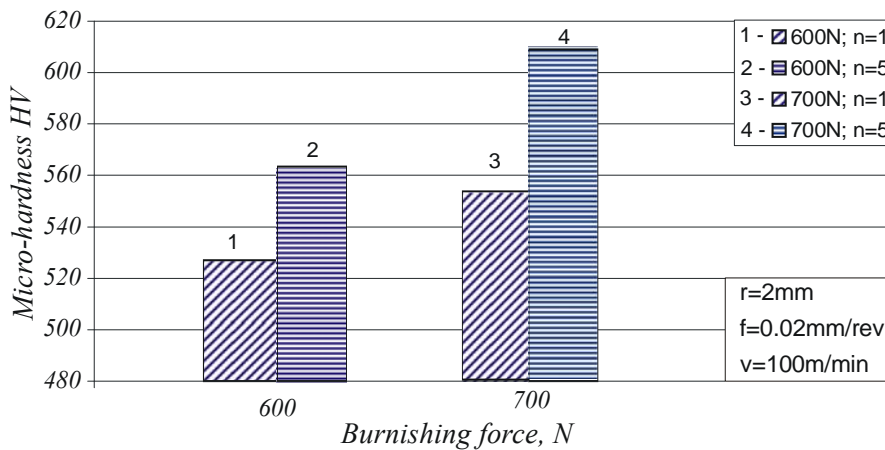


Fig. 8. Some combination providing high micro-hardness

3.2. Optimization under maximum surface micro-hardness criterion

Based on a one-factor-at-a-time study, it can be concluded that from the main parameters of the DB process, the radius of the deforming diamond, burnishing force and feed rate significantly affect the micro-hardness. The effect of number of passes is also noticeable. Fig. 8 shows the effect of some combinations of these parameters. Obviously, the combination of minimum radius, maximum force, minimum feed and number of passes $n = 5$ will lead to maximum surface micro-hardness: the initial micro-hardness (after turning and fine turning) from 366 HV increases to 609 HV through diamond burnishing, i.e., the increase is 66.4%.

4. CONCLUSIONS

The influence of diamond burnishing of chromium-nickel austenitic stainless steel on the surface micro-hardness obtained is studied. The following conclusions can be made:

- The workpiece diameter and burnishing velocity weakly affect on the surface micro-hardness
- The radius of the deforming diamond and feed rate affect the most on the surface micro-hardness, followed by the burning force and the number of passes.
- The combination of minimum radius, maximum burnishing force and minimum feed rate, implemented via five passes, leads to maximum surface micro-hardness: the initial micro-hardness (after turning and fine turning) from

366 HV increases to 609 HV through diamond burnishing, i.e., the increase is 66.4%.

ACKNOWLEDGMENT

This work was supported by the European Regional Development Fund within the OP „Science and Education for Smart Growth 2014-2020”, Project CoC “Smart Mechatronics, Eco- and Energy Saving Systems and Technologies”, №BG05M2OP001-1.002-0023.

REFERENCES

- [1] Balevski A.T. Metal-knowledge. Technika, Sofia, 1988 (in Bulgarian)
- [2] Cao Y., Maistro G., Norell M., Prez-Garsia S.A., Nyborg L. Multi-technique characterization of low-temperature plasma nitrided austenitic AISI 304L and AISI 904L stainless steel. *Surface and Interface Analysis* 46 (2014) 856-860
- [3] Flis J., Kuczynska M. Effect of low-temperature plasma nitriding on corrosion of 304L stainless steel in sulfate and chloride solutions. *Journal of the Electrochemical Society* 151(11) (2004) B573-B580
- [4] Kuczynska-Wydorska M., Flis J. Corrosion and passivation of low-temperature nitrided AISI 304L and 316L stainless steels in acidified sodium sulphate solution. *Corrosion Science* 50 (2008) 523-533
- [5] Qin X., Guo X., Lu J., Chen L., Qin J., Lu W. Erosion-wear and intergranular corrosion resistance properties of AISI 304L austenitic stainless steel after low-temperature plasma nitriding. *Journal of Alloy and Compounds* 698 (2017) 1094-1101
- [6] Cao Y., Ernst F., Michal G.M. Colossal carbon supersaturation in austenitic stainless steels carburized at low temperature. *Acta Materialia* 51 (2003) 4171
- [7] Mitra A., Srivastava P.K., De P.K., Bhattacharya D.K., Jiles D.C. Ferromagnetic properties of deformation-induced martensite transformation in AISI 304 stainless steel. *Metall Mater Trans A* 35 (2004) 599-605
- [8] Hedayati A., Najafizadeh A., Kermanpur A., Forouzan F. The effect of cold rolling regime on microstructure and mechanical properties of AISI 304L stainless steel. *J Mater Process Technol* 210 (2010) 1017-1022
- [9] Kim Y.S., Lee D.J., Kang Y.J., Pak S.J. Effect of solution annealing on alpha prime martensitic microstructure of cold rolled AISI 316L stainless steel. *Aspects in Mining and Mineral Science* 4(1) (2019) 481-484
- [10] Kumar B.R., Singh A.K., Das S., Bhattacharya D.K. Cold rolling texture in AISI 304 stainless steel. *Materials Science and Engineering A364* (2004) 132-139
- [11] Kurc-Lisiecka A., Kalinowska-Ozgowicz E. Structure and mechanical properties of austenitic steel after cold rolling. *Journal of Achievements in Materials and Manufacturing Engineering* 44(2) (2011) 148-153
- [12] Li X., Wei Y., Wei Z., Zhou J. Effect of cold rolling on microstructure and mechanical Properties of AISI 304N stainless steel. *IOP Conf. Series: Earth and Environmental Science* 252 (2019) 022027
- [13] Chen X.H., Lu J., Lu L., Lu K. Tensile properties of a nanocrystalline 316L austenitic stainless steel. *Scripta Materialia* 52 (2005) 1039-1044
- [14] Milad M., Zreiba N., Elhalouani F., Barada C. The effect of cold work on structure and properties of AISI 304 stainless steel. *J Mater Process Technol* 203 (2008) 80-85
- [15] Singh R., Goel S., Verma R., Jayaganthan R., Kumar A. Mechanical behaviour of 304 austenitic stainless steel processed by room temperature rolling. *IOP Conf. Series: Materials Science and Engineering* 330 (2018) 0120017
- [16] Suyitno, Arifvianto B., Widodo T.D., Mahardika M., Dewo P., Salim U.A. Effect of cold working and sandblasting on the microhardness, tensile strength and corrosion resistance of AISI 316L stainless steel. *Int J Miner Metall Mater* 19(12) (2012) 1093-1099
- [17] Tanhaei S., Gheisari K., Zaree S.R.A. Effect of cold rolling on the microstructural, magnetic, mechanical, and corrosion properties of AISI 316L austenitic stainless steel. *International Journal of Minerals, Metallurgy, and Materials* 25(6) (2018) 630-640
- [18] Tavares S.S.M., Gunderov D., Stolyarov V., Neto J.M. Phase transformation induced by severe plastic deformation in the AISI 304L stainless steel. *Materials Science and Engineering A358* (2003) 32-36
- [19] Wang Y-N., Chen J., Peng H-B., Wen Y-H. Shape memory effect induced by stress-induced α' martensite in a metastable Fe-Cr-Ni austenitic stainless steel. *Acta Metall. Sin. (Engl. Lett.)* 30(6) (2017) 513-520
- [20] Zimmerman M., Grigorescu A., Müller-Bollenhagen C., Christ H-J. Influence of deformation-induced alpha prime martensite on the crack initiation mechanism in a metastable austenitic steel in HCF and VHCF regime. 13th International Conference on Fracture, June 16-21, 2013, Beijing, China, *Proceedings*, 7 (2013) 5208-5216
- [21] Dyl T., Wijata M., Kuśmierska-Matyszczyk W. The slide broaching burnishing and the influence of deformation on roughness of 314L stainless steel sleeves. *Scientific Journal of Gdynia Maritime University*, 116 (2020) 15-28
- [22] Shi Y., Shen X., Xu G., Xu C., Wang B., Su G. Surface integrity enhancement of austenitic stainless steel treated by ultrasonic burnishing with two burnishing tips. *Archives of Civil and Mechanical Engineering*, 20(3) (2020) 1-17
- [23] Varga G., Ferencsik V. Experimental examination of surface micro-hardness improvement ratio in burnishing of external cylindrical workpieces. *Cutting & Tools in Technological System* 93 (2020) 114-121
- [24] Konefal K., Korzynski M., Byczkowska Z., Korzynska K. Improved corrosion resistance of stainless steel X6CrNiMoTi17-12-2 by slide diamond burnishing. *Journal of Materials Processing Technology* 213 (2013) 1997-2004
- [25] Korzynski M., Dudek K., Kruczek B., Kocurek P. Equilibrium surface texture of valve stems and burnishing method to obtain it. *Tribology International* 124 (2018) 195-199
- [26] Korzynski M., Dudek K., Palczak A., Kruczek B., Kocurek P. Experimental models and correlations between surface parameters after slide diamond burnishing. *Measurement Science Review* 18(3) (2018) 123-129
- [27] Maximov J.T., Duncheva G.V., Anchev A.P., Ganey N., Amudjev I.M., Dunchev V.P. Effect of slide burnishing method on the surface integrity of AISI 316Ti chromium-nickel steel. *J Braz. Soc. Mech. Sci. Eng.* 40 (4) (2018) 1-14
- [28] Okada M., Shinya M., Matsubara H., Kozuka H., Tachiya H., Asakawa N., Otsu M. Development and characterization of diamond tip burnishing with a rotary tool. *Journal of Materials Processing Technology* 244 (2017) 106-115
- [29] Maximov J.T., Duncheva G.V., Anchev A.P., Ganey N., Dunchev V.P. Effect of cyclic hardening on fatigue performance of slide burnishing components made of low-alloy medium carbon steel, *Fatigue Fract Eng Mater Struct* 42(6) (2019) 1414-1425